Alumina Passives Using the Interconnect Layer of Metal-Embedded Chip Assembly Processing

José Estrada, Gregor Lasser, Mauricio Pinto, Florian Herrault* and Zoya Popović
University of Colorado, Boulder, Colorado, 80309, USA (Email: jose.estrada@colorado.edu)
*HRL Laboratories, Malibu, California, 90265, USA

***Abstract*—This paper describes the additional design dimension of a new heterogeneous packaging process, referred to as Metal-Embedded Chip Assembly (MECA). The interconnect layers of the process can be used as an additional degree of freedom for design and manufacturing of passive circuits for integrated RF front-ends. Transmission lines designed with the interconnect layer, referred to as bridge lines, with up to 35 % higher characteristic impedances than their microstrip counterpart, are validated by measurements up to 25 GHz. An X-band Lange coupler with 3.9 GHz bandwidth is designed using MECA interconnects, with accurate bridge placement. Broadband measurements from 0 to 25 GHz show good agreement with simulations.**

***Index Terms*—Heterogeneous integration, interconnects, Lange coupler, high impedance, microstrip, alumina, MECA.**

I. Introduction

Heterogeneous integration is gaining increased interest for miniaturized RF front-ends [1]. The goal is to enable integration of RF compound semiconductor (GaAs, GaN and InP) components, with digital and analog CMOS components [2], [3] and low-cost high-performance passives implemented in alumina, aluminum nitride [4], silicon [5] or glass.

HRL's Metal Embedded Chip Assembly (MECA) [4], is a technique for heterogeneous integration that provides an excellent thermal and RF ground. The MECA concept consists of integrating chips into a copper heat spreader block within the thickness of a silicon interposer wafer. By making intimate contact between the backside of the chips and the heat spreader, while eliminating any thermal interface materials, the thermal management characteristics are improved over traditional technologies. This process offers a lithography-based interconnect layer that replaces bond wires and other packaging techniques.

In this work we address the heterogeneous integration of low cost high performance passives implemented in alumina. We demonstrate a new type of microstrip line and a Lange coupler to showcase the use of the MECA interconnects as an additional degree of freedom for the design of microwave circuits, combined with alumina microstrip structures that can be manufactured in a simple and economic way. The higher characteristic impedance microstrip lines, with the geometry shown in Fig. 1 are discussed in the next section. Such lines are useful for quasi-MMIC design [6] where the matching, combining and bias networks do not use expensive semiconductor area. As an example an 7.9 to 11.8 GHz Lange coupler with bridges built with MECA interconnects is demonstrated.

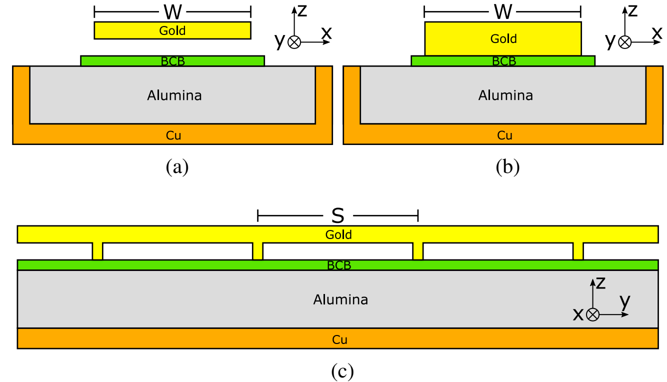

Fig. 1. Bridge-line microstrip geometry: (a) strip cross-section; (b) post cross-section; and (c) side cross-section. W is the strip width and S is the section between two post centers. In this work, we use 254 μm alumina, 3 μm BCB, 5 μm air, 5 μm gold thickness, 20 μm post length and $S = 220\,\mu$m.

The MECA process is illustrated in Fig. 2. Chips fabricated in different technologies are mounted face-down on a temporary carrier wafer, followed by bonding to a metallized interposer Si wafer with etched cavities. The copper heat spreader is then electroformed into the cavities, and the MECA wafer released from the temporary carrier wafer and flipped. After this step, the chips are embedded in the copper heat spreader which makes the MECA wafer. Finally, single-layer air-bridge Au MECA interconnects for chip-to-chip, chip-to-body, and intra-chip electrical connections are fabricated, as shown in more detail in Fig. 1c. In this process, the minimum line width W is 20 μm and the maximum bridge length S is 500 μm, determining the main design parameters.

II. Bridge-Line Microstrip

Inhomogeneous microstrip lines with an air layer can be realized with higher characteristic impedances, due to the decrease in capacitance per unit length [7]. To implement these bridge-lines, support posts are required for structural integrity, as shown in Fig. 1c. A section of transmission line is defined from the center of a bridge to the center of the next one and denoted with the distance S shown in Fig. 1c. The phase velocity is given by

978-1-5386-7333-1/18/$31.00 ©2018 IEEE

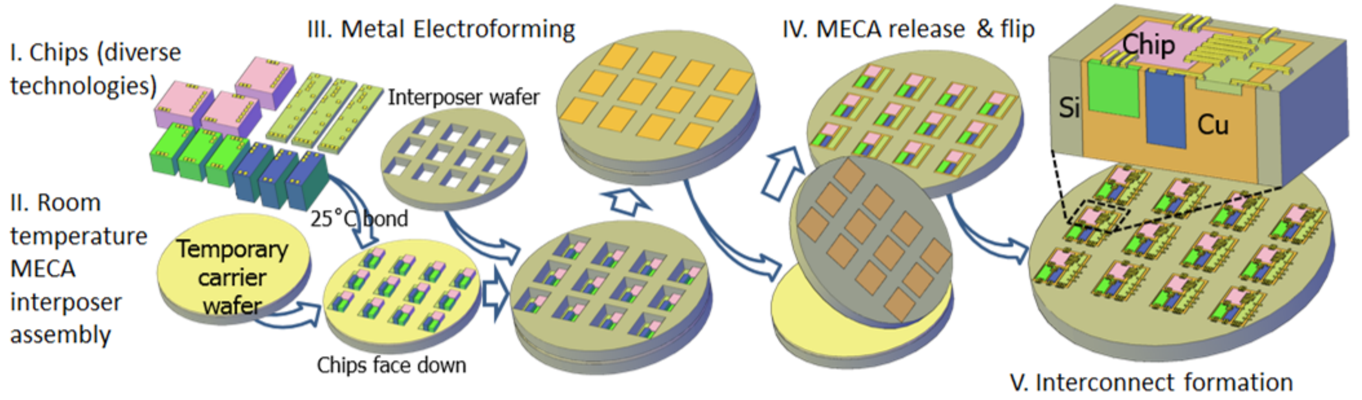

Fig. 2. High-level illustration of the Metal Embedded Chip Assembly (MECA) process flow.

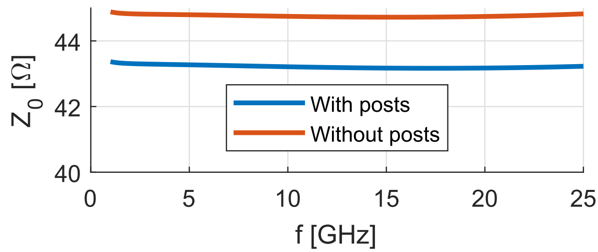

Fig. 3. Simulated effect of posts in the characteristic impedance of a line with 254 μm thick alumina, 3 μm BCB, 5 μm air, 5 μm gold thickness, 20 μm post length and $S = 220\,\mu$m.

$$v_p = \lambda f = \frac{S}{\Delta t},$$

where λ is the guided wavelength, f is the frequency and Δt is the group delay of the section. The frequencies where the length of this section is P % of the wavelength are given by

$$f = \frac{\left(\frac{P\lambda}{100}\right)}{\lambda \Delta t} = \frac{P}{100\Delta t}.$$

Full-wave electromagnetic simulations (using Ansys HFSS) show that the group delay for one section of line is around $\Delta t = 2$ ps, resulting in $f = 5P$ GHz. From here it can be seen that frequencies under 25 GHz have a section length that is smaller than 5 % of the wavelength and therefore the bridge-line behaves as a distributed transmission line. The upper frequency limit for uniform transmission line behavior will be determined by the resonant frequency of the posts and their periodicity, found by simulations to be around 250 GHz for this $S = 220\mu$m.

The periodic posts that provide structural stability also increase the capacitance per unit length of the line therefore decreasing the characteristic impedance. For a maximum operating frequency well above 25 GHz and high characteristic impedance these posts should be made as small and far apart as possible. For example, the simulated characteristic impedance of a bridge-line with 254 μm thick alumina, 3 μm BCB, 5 μm air, 5 μm gold thickness and line width of 330 μm decreases from 45 Ω to 43 Ω when the posts (20 μm post length and $S = 220\,\mu$m) are included, Fig. 3.

TABLE I
REALIZABLE IMPEDANCES WITH DIFFERENT MICROSTRIP WIDTHS BASED ON FULL-WAVE EM SIMULATIONS AND FIG. 1.

Line type	$W = 400\,\mu$m	$W = 20\,\mu$m
Microstrip	38 Ω	108 Ω
Bridge-Line Microstrip	43 Ω	147 Ω

The range of impedances that can be obtained on an alumina substrate with 254 μm thickness and 5 μm gold strips can be seen in Table I. This table also shows the realizable impedances in the same substrate using bridge-lines that have 3 and 5 μm BCB and air layers, respectively, as well as posts with 20 μm post length and $L = 220\,\mu$m. Bridge-line microstrips can thus be used to increase the maximum realizable impedance from 108 Ω to 147 Ω (a 35 % increase) for the same line width.

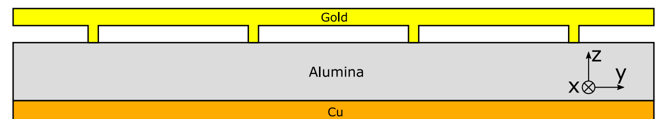

Fig. 4. Bridge-line microstrip geometry without the BCB layer.

III. Experimental Results

Lines with 50 and 90 Ω characteristic impedance were designed to have respective widths of 116 and 350 μm. Due to the experimental nature of the MECA process, in this particular run the BCB layer was omitted, resulting in bridges dropped in height by the BCB thickness, Fig. 4 shows the resulting geometry. As a result, the line impedances dropped to $Z_0 = 43\,\Omega$ and $Z_0 = 83\,\Omega$ and the fabricated structures can be seen in Fig. 5. These bridge-lines lines have 12 sections with posts that are 5 μm tall. The removal of the BCB layer should not substantially affect the performance of the lines and

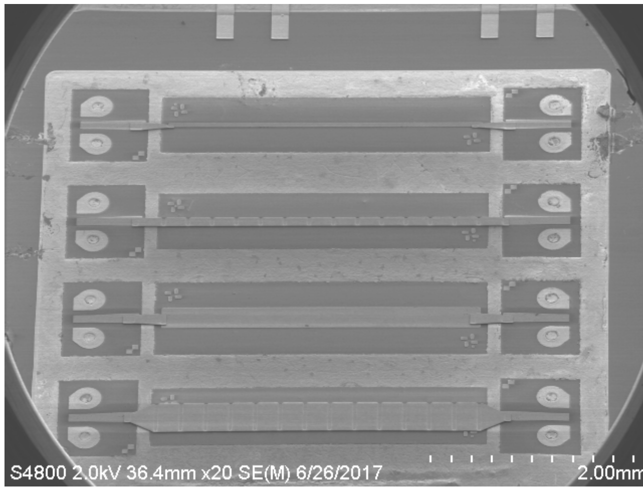

Fig. 5. Photograph of the fabricated test transmission lines. The second and fourth lines are bridge line microstrip, the posts can be seen in this photo. The launchers are alumina ProbePoint™ 0503.

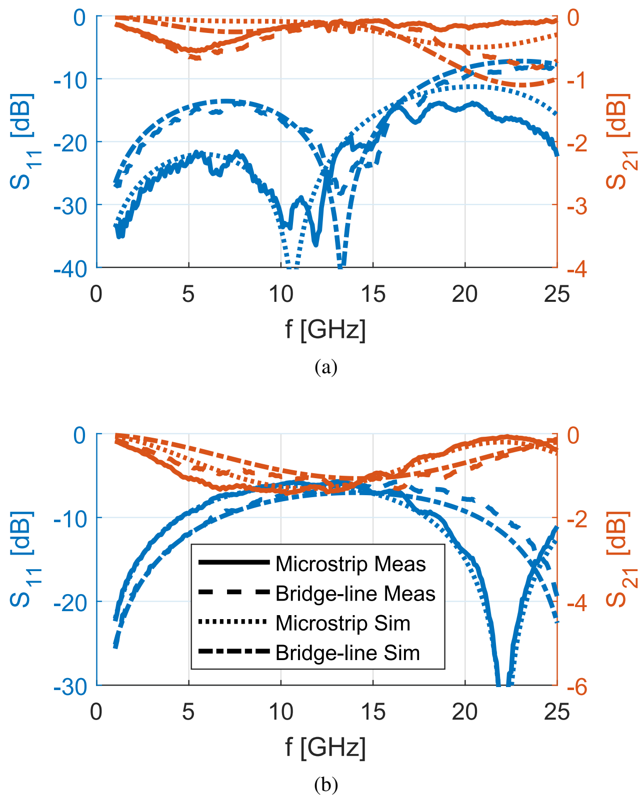

Fig. 6. S-parameters of the (a) 43 Ω line with $W = 240\,\mu$m for the microstrip and $W = 330\,\mu$m for the bridge line, and (b) 83 Ω line with $W = 46\,\mu$m for the microstrip and $W = 96\,\mu$m for the bridge line.

Fig. 6 shows a comparison of the measurement and simulation results. For these simulations the interconnects to the lines are also modeled and no BCB layer is used.

The interconnect layer of the MECA heterogeneous integration process can also be used to complete simple single layer circuits designed in alumina. For example, a Lange coupler requires a second metal layer often implemented with bond wires, which can be replaced by a short bridge-line section. The fabricated Lange coupler can be seen in Fig. 7 with measured results shown in Fig. 8. The coupler has a frequency range from 7.9 to 11.8 GHz over which the amplitude balance is less than 1 dB and the phase balance is within 90.7 ° and 91.5 °. Insetion loss is 0.5 dB, return loss and isolation are both greater than 22.5 dB and 24.6 dB, respectively.

In summary, the interconnect layer of heterogeneous integration processes gives an additional design degree of freedom that can improve performance of passive components necessary in miniaturized RF front ends.

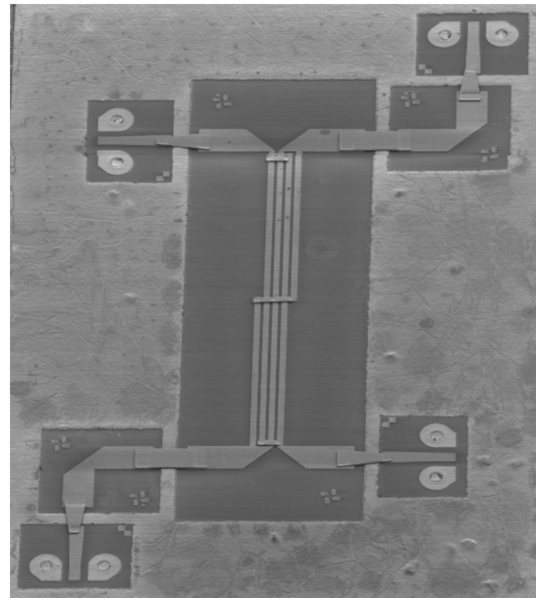

Fig. 7. Photograph of the fabricated Lange coupler (total length 5 mm). The launchers are alumina ProbePoint™ 0503. Alumina L-sections were used to enable 4-port on wafer probing of the coupler, these are deembedded in all the shown measurements.

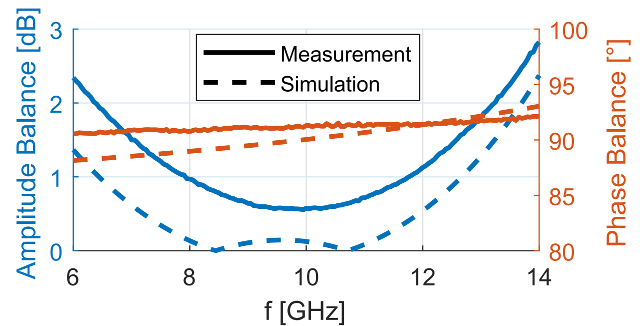

Fig. 8. Lange coupler measurement results. $RL = 22.5\,$dB, $IL = 0.5\,$dB and $I = 24.6\,$dB.

References

[1] D. S. Green *et al.*, "A revolution on the horizon from darpa: Heterogeneous integration for revolutionary microwave/millimeter-wave circuits at darpa: Progress and future directions," *IEEE Microwave Magazine*, vol. 18, no. 2, pp. 44–59, March 2017.

[2] J. C. Li *et al.*, “Heterogeneous wafer-scale integration of 250nm, 300ghz inp dhbts with a 130nm rf-cmos technology,” in *2008 IEEE International Electron Devices Meeting*, Dec 2008, pp. 1–3.

[3] Y. C. Wu *et al.*, “Inp hbt/gan hemt/si cmos heterogeneous integrated q-band vco-amplifier chain,” in *2015 IEEE Radio Frequency Integrated Circuits Symposium (RFIC)*, May 2015, pp. 39–42.

[4] A. Margomenos *et al.*, “X band highly efficient gan power amplifier utilizing built-in electroformed heat sinks for advanced thermal management,” in *2013 IEEE MTT-S International Microwave Symposium Digest (MTT)*, June 2013, pp. 1–4.

[5] M. Sato *et al.*, “Heterogeneous integration of microwave gan power amplifiers with si matching circuits,” *IEEE Transactions on Semiconductor Manufacturing*, vol. 30, no. 4, pp. 450–455, Nov 2017.

[6] M. Ayad *et al.*, “Single and dual input packaged 5.5-6.5ghz, 20w, quasi-mmic gan-hemt doherty power amplifier,” in *2017 IEEE MTT-S International Microwave Symposium (IMS)*, June 2017, pp. 114–117.

[7] M. E. Goldfarb and V. K. Tripathi, “The effect of air bridge height on the propagation characteristics of microstrip,” *IEEE Microwave and Guided Wave Letters*, vol. 1, no. 10, pp. 273–274, Oct 1991.